

Title	Self-stabilizing Human-Like Motion Control Framework for Humanoids Using Neural Oscillators
Author(s)	Yang, Woosung; Chong, Nak Young; Ra, Syungkwon; Bae, Ji-Hun; You, Bum Jae
Citation	Lecture Notes in Computer Science, 5754/2009: 512-525
Issue Date	2009-09-19
Type	Journal Article
Text version	author
URL	http://hdl.handle.net/10119/9517
Rights	This is the author-created version of Springer, Woosung Yang, Nak Young Chong, Syungkwon Ra, Ji-Hun Bae and Bum Jae You, Lecture Notes in Computer Science, 5754/2009, 2009, 512-525. The original publication is available at www.springerlink.com , http://dx.doi.org/10.1007/978-3-642-04070-2_57
Description	Emerging Intelligent Computing Technology and Applications, 5th International Conference on Intelligent Computing, ICIC 2009, Ulsan, South Korea, September 16-19, 2009. Proceedings



Self-stabilizing Human-like Motion Control Framework for Humanoids Using Neural Oscillators

Woosung Yang¹, Nak Young Chong², Syungkwon Ra¹, Ji-Hun Bae¹,
Bum Jae You¹

¹ Center for Cognitive Robotics Research, Korea Institute of Science and Technology, Seoul,
Korea

{wsyang, sykra, joseph and ybj}@kist.re.kr

² School of Information Science, Japan Advanced Institute of Science and Technology,
Ishikawa, Japan
nakyoun@jaist.ac.jp

Abstract. We propose an efficient and powerful alternative for adaptation of human motions to humanoid robots keeping the bipedal stability. For achieving a stable and robust whole body motion of humanoid robots, we design a biologically inspired control framework based on neural oscillators. Entrainments of neural oscillators play a key role to adapt the nervous system to the natural frequency of the interacted environments, which show superior features when coupled with virtual components. The coupled system allows an unstable system to stably move according to environmental changes. Hence the feature of the coupled system can be exploited for sustaining the bipedal stability of humanoid robots. Also based on this, a marionette-type motion conversion method to adapt captured motions to a humanoid robot is developed owing that there are the differences in capabilities of dynamics and kinematics between a robot and a human. Then this paper discuss on how to stably show human motions with a humanoid robot. We verify that a real humanoid robot can successfully sustain the bipedal stability exhibiting captured whole body motions from various simulations and experiments.

Keywords: Humanoid robot, Neural oscillator, Biologically inspired robot control, Bipedal control, Human-like motion, Imitation

1 Introduction

Researches on human-like motion have been paid attention to achievement of real or virtual human-like robots in the humanoid robot community for the last decade. Considerable efforts have been mainly devoted to how to solve a highly nonlinear nature of robot dynamics and disturbances from an uncertain environment. In particular, since humanoid robots have a large number of degrees-of-freedom and should maintain the bipedal stability, efficient motion generation and control which the stability problem is considered still remain challenging.

From a practical viewpoint, imitation for human-like motion generation of humanoid robots is considered as a powerful means of enhancing pattern generation

competence. Many researchers have studied efficient imitation models to obtain reliable motion data in noisy stochastic environments [1]-[5]. Especially, Inamura *et al.* devised the mimesis model based on HMM which can imitate the motion of others and abstract the time-series motion patterns as symbol representation [1]. Samejima *et al.* suggested a special framework MOSAIC, where plural dynamics and inverse dynamics are implemented to predict and control motions [4]-[5]. Also, for human motion generation, Yamane and Nakamura computed the interacting dynamics of structure-varying kinematic chains by incorporating an efficient collision/contact model [6]-[7]. Yang *et al.* showed stable bipedal motions of humanoid robots using the proposed SAA through imitation learning [8]-[10].

Although recent progress in imitation learning for human motion generation has yielded notable results in many cases, a unified approach to behavior generation of humanoid robots remains so far largely undetermined. Particularly, only a few approaches have been reported concerning imitation methods that requires effect reproduction through close interaction with the environment. On the other hand, relating to realizing the stable bipedal locomotion, these efforts include such approaches as the zero moment point criterion [11]-[12], the linear inverted pendulum mode [13], virtual model control [14], and biologically inspired approaches [15]-[16].

Several methods do not depend heavily on the predefined reference patterns. However, the motion data captured from humans may not be straightforwardly used owing that these mainly discuss some forms of pattern generation and tracking control for the locomotion of humanoid robots. Moreover, many existing methods require substantial constraints for sustaining the bipedal stability. This causes confliction between the stability problem and imitation motion generation of humanoid robots. Consequently, it is difficult to attain an appropriate human-like motion through imitation with humanoid robots.

This work addresses how to exhibit human-like movements stabilizing bipedal motions. For achieving both of them, the authors propose a marionette-type motion conversion method which helps properly generate human-like motions from captured motion data for humanoid robots. Due to using forward dynamics and virtual force constraint, our motion adaptor shows superior features in mathematical computation and acquisition of more smoothed marker data. In addition, the neural oscillator based self-stabilizer allows bipedal robots to easily embody an appropriate bipedal motion corresponding to various desired the ZMP patterns sustaining the bipedal stability. Also this requires that humanoid robots should maintain the stability even in an unknown disturbance without an additional controller owing to an entrainment property of the neural oscillator. It is verify through simulations and experiments that the proposed approach yields a robust and efficient control of human-like motions.

1 Neural Oscillator based Control

Our work is motivated by studies and facts of biologically inspired locomotion control employing oscillators. Especially, the basic motor pattern generated by the Central Pattern Generator (CPG) of inner body of human or animal is usually modified by sensory signals from motor information to deal with environmental

disturbances. Similar to the sensory system of human or animal, the neural oscillators are entrained with external stimuli at a sustained frequency. They show stability against perturbations through global entrainment between the neuro-musculo-skeletal systems and the ground [17]. Thus, neural oscillators have been applied to the CPG of humanoid robots with rhythmic motions [18]-[19].

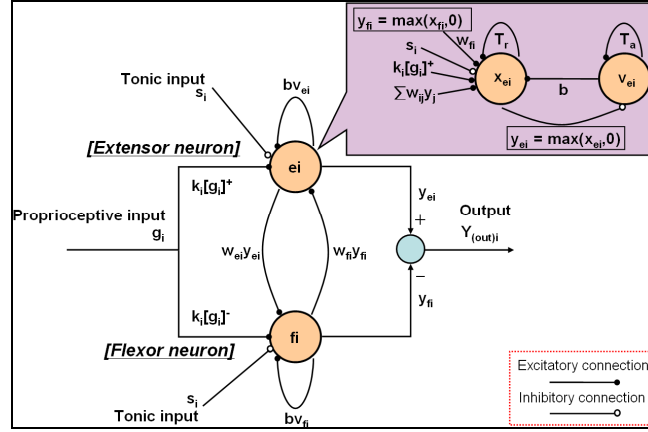


Fig. 1. Schematic diagram of Matsuoka's Neural Oscillator

$$\begin{aligned}
 T_r \dot{x}_{ei} + x_{ei} &= -w_{fi} y_{fi} - \sum_{j=1}^n w_{ij} y_j - bv_{ei} - \sum k_i [g_i]^+ + s_i \\
 T_a \dot{v}_{ei} + v_{ei} &= y_{ei} \\
 y_{ei} &= [x_{ei}]^+ = \max(x_{ei}, 0) \\
 T_r \dot{x}_{fi} + x_{fi} &= -w_{ei} y_{ei} - \sum_{j=1}^n w_{ij} y_j - bv_{fi} - \sum k_i [g_i]^- + s_i \\
 T_a \dot{v}_{fi} + v_{fi} &= y_{fi} \\
 y_{fi} &= [x_{fi}]^+ = \max(x_{fi}, 0), (i = 1, 2, \dots, n)
 \end{aligned} \tag{1}$$

where x_{ei} and x_{fi} indicate the inner state of the i -th neuron for $i=1 \sim n$, which represents the firing rate. Here, the subscripts 'e' and 'f' denote the extensor and flexor neurons, respectively. $v_{e(f)i}$ represents the degree of adaptation and b is the adaptation constant or self-inhibition effect of the i -th neuron. The output of each neuron $y_{e(f)i}$ is taken as the positive part of x_i and the output of the oscillator is the difference in the output between the extensor and flexor neurons. W_{ij} is a connecting weight from the j -th neuron to the i -th neuron: w_{ij} are 0 for $i \neq j$ and 1 for $i=j$. $w_{ij} y_j$ represents the total input

from the neurons arranged to excite one neuron and to inhibit the other, respectively. Those inputs are scaled by the gain k_i . T_r and T_a are the time constants of the inner state and the adaptation effect, respectively, and s_i is an external input with a constant rate. $W_{e(f)i}$ is a weight of the extensor neuron or the flexor neuron and g_i indicates a sensory input.

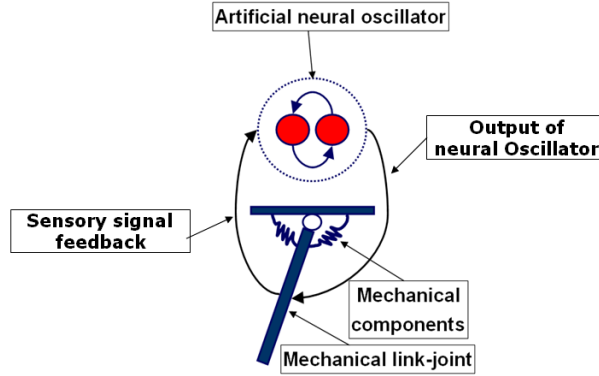


Fig. 2. Mechanical system coupled to the neural oscillator

For implementing the neural oscillator, the oscillator should be coupled to the dynamic system that closely interacts with environments. This enables a robot to adapt to changing environment conditions. For simplicity, we employ a general 2nd order mechanical system connected to the neural oscillator as seen in Fig. 2. The desired torque signal to the joint can be given by

$$\tau = p(\theta_{od} - \theta) - v\dot{\theta}, \quad (2)$$

where p is the position gain, v the velocity gain, θ the actual angle, and θ_{od} the desired angle of the joint, respectively. Specifically, θ_{od} is the output of the neural oscillator that produces rhythmic commands of the joint of the mechanical system. The neural oscillator follows the sensory signal from the joint, thus the output of the neural oscillator may change corresponding to the sensory input. This is what is called “entrainment” that can be considered as the tracking of sensory feedback signals so that the mechanical system can exhibit adaptive behavior interacting with the environment [20]. The key to implementing this method is how to incorporate the input signal’s amplitude information as well as its phase information.

3 The Control Model for Bipedal Stability

It would be advantageous if humanoid robots can maintain its stability without using sophisticated controllers. The proposed control approach involves a new application

of the interaction between neural oscillators and virtual components to the bipedal stability control of humanoids. This allows humanoid robots to adapt their motions through entrainment responding to unknown disturbances. Now we explain how to embody the stable single support or double phases of humanoid robots corresponding to the lower legged motion generation. In order to maintain stability, the neural oscillator plays an important role by controlling the trajectory of the COM in phase with the ZMP input.

Note that the single support phases bring about significant effects on the landing stability of swing legs that may cause an unexpected perturbation with imperfect contact. To avoid this, we consider a virtual inverted pendulum model coupled to such a virtual mechanical component as a spring and damper and the neural oscillator, as seen in Fig. 7 for generating an appropriate rolling and pitching motion. The coupled model enables the inverted pendulum to stably move in a frontal and sagittal plane according to a desired ZMP trajectory sustaining the stability. For technically implementing this to a humanoid robot, we simplified the bipedal walking model as a well known linear inverted pendulum model.

Assuming that θ , the inclined angle between the vertical axis and the pendulum in Figs. 3 (a) and (b), is small enough and linearized near 0, the dynamic equations of the coupled inverted pendulum in the pitching and rolling direction are given by

$$\begin{bmatrix} \ddot{x} \\ \ddot{y} \end{bmatrix} = \frac{G}{l} \begin{bmatrix} x-u_x & 0 \\ 0 & y-u_y \end{bmatrix} + \begin{bmatrix} F_x \\ F_y \end{bmatrix}, \quad (3)$$

where x and y are the displacement of the pendulum in the pitching and rolling direction, respectively. l is the length of the pendulum, and u is the position of the massless cart of the pendulum. Note that the subscriptions, 'x' and 'y', indicate the pitching and rolling direction in the entire paper, respectively. G is the gravitational constant. F_x and F_y indicates the force that should be applied to the Center of Mass (COM) of the pendulum in the pitching and rolling direction, respectively.

If the desired ZMP trajectory, u_{y_s} , is given in Eq. (3), a stably periodic motion of the COM of the pendulum is generated in terms of the coupled neural oscillator with state feedback [16] (see Fig. 3(c)). If a mechanical system is coupled to the neural oscillator, the dynamic stability is improved [20]. Hence, a stable limit cycle behavior is induced and the periodic COM motion is achieved by the impedance control of the virtual components. Accordingly, F_x and F_y in Eq. (4) are given by

$$\begin{bmatrix} F_x \\ F_y \end{bmatrix} = \frac{1}{ml} \left\{ 2k_s \left(\begin{bmatrix} h_x & 0 \\ 0 & h_y \end{bmatrix} \begin{bmatrix} \theta_{o,x} \\ \theta_{o,y} \end{bmatrix} - \begin{bmatrix} P_x & 0 \\ 0 & P_y \end{bmatrix} \begin{bmatrix} x \\ y \end{bmatrix} \right) - \begin{bmatrix} D_x & 0 \\ 0 & D_y \end{bmatrix} \begin{bmatrix} \dot{x} \\ \dot{y} \end{bmatrix} + \begin{bmatrix} i_{p,x} & 0 \\ 0 & i_{p,y} \end{bmatrix} \begin{bmatrix} x_d - x \\ y_d - y \end{bmatrix} - \begin{bmatrix} i_{v,x} & 0 \\ 0 & i_{v,y} \end{bmatrix} \begin{bmatrix} \dot{x} \\ \dot{y} \end{bmatrix} \right\}, \quad (4)$$

where k_s is the stiffness coefficient. h_x and h_y are the output gains of each neural oscillator in the pitching and rolling direction, respectively. P and D are the gains of

state feedback, and $i_{p,x}$, $i_{p,y}$, $i_{v,x}$ and $i_{v,y}$ are the gains of the impedance controller. In the proposed controller, $\theta_{o,x}$ and $\theta_{o,y}$ denote the outputs of the neural oscillators coupled to the COM of the inverted pendulum corresponding to the individual direction as illustrated in Eq. (2). x_d and y_d denote the desired ZMP inputs.

The current COM position and velocity of the humanoid robot are obtained again by Eq. (3). For a stable pitching and rolling motion corresponding to an arbitrary ZMP input, F_x and F_y in Eq. (4) are transformed into joint torques using the Jacobian that needs to be applied to each joint of both legs of humanoid robots. For example, as illustrated in Fig. 3 (b), the humanoid robot exhibits stable rolling motion satisfying the desired ZMP. Also the stable pitching motion in Fig. 3 (a) can be attained in the same way.

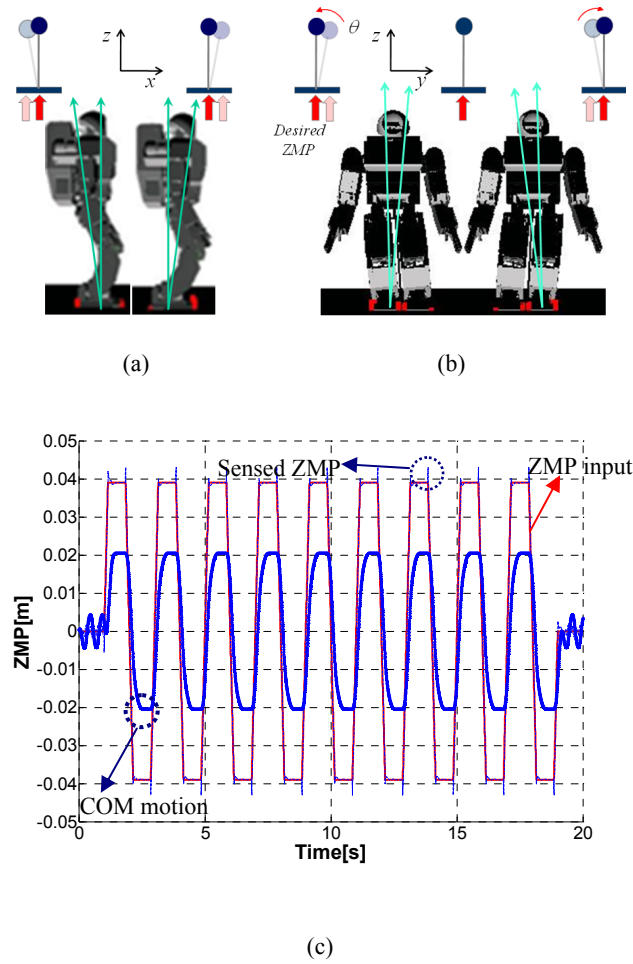


Fig. 3. Simulation result with respect to the stable pitching (a) and rolling (b) motion of the humanoid robot, (c) Plot of the COM motion of humanoid robot in the rolling direction according to the ZMP input

4 Implementation and Basic Tests of the Coupled Model

This section describes how to embody the bipedal motion of a real humanoid robot using the proposed control scheme to guarantee the stability on the single and double support phases. The humanoid robot in Fig. 4, developed by KIST, is used to test and evaluate the proposed controller. It has 35 degrees of freedom (DOF): 6 in each arm, 6 in each leg, 4 in each hand, 2 in neck, and 1 in waist. It's 150cm high and weighs about 67kg. The robot is equipped with a stereo camera, a microphone, four force/torque sensors, and a pose sensor

We firstly performed numerical simulations to verify the proposed control method. In this simulation, we use the humanoid robot simulator, named *Simstudio*, developed in *SimLab* co. Prior to experiment on human-like whole body motion, we test a few motions during the double support and single support phases, since the analysis of those supporting phases is essential for bipedal walking or other movements. Also, we investigate through experiments of following section whether the output of the neural oscillator is adapted to the dynamic motion of the humanoid robot.

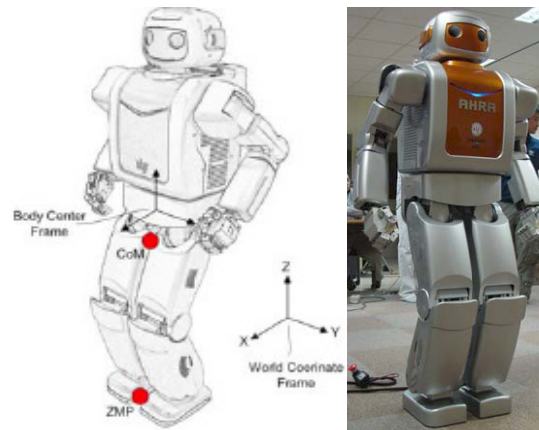


Fig. 4. KIST Humanoid robot

After implementing the control algorithm to the *Simstudio*, we acquired the simulation results of the hip positions during rolling and pitching as seen in Figs. 5 and 6. The hip positions are generated appropriately by an arbitrarily defined ZMP input seen in Figs. 5 and 6. This implies that the proposed control method in section 3 works properly. The dashed line in the figures indicates the input pattern of the desired ZMP. The solid lines of Figs. 5 and 6 show the COM of the humanoid robot with regard to the rolling and pitching motions, respectively. Remarkably, the dotted line in Fig. 5 and the dash-dotted line in Fig. 6 are the outputs of the neural oscillators, when the humanoid robot periodically moves in the lateral and sagittal planes. The COM motion of the humanoid robot fed again is considered as the sensory signal of the neural oscillator. Then the outputs of neural oscillator entrain that of the humanoid robot and drive the humanoid robot corresponding to the sensory input appropriately as a torque input. From these results, it can be observed that the neural oscillator

causes the self-adapting motion to follow the sensory input. Consequently, we note that this leads the adaptive motion of humanoid robots to maintain the bipedal stability even under an unknown disturbance.

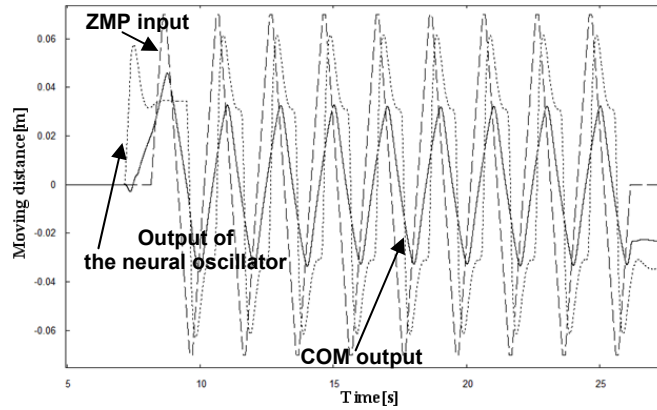


Fig. 5. Input ZMP profile (dashed line), the output of the COM position (solid line) and the output of the neural oscillator in the rolling motion (dotted line)

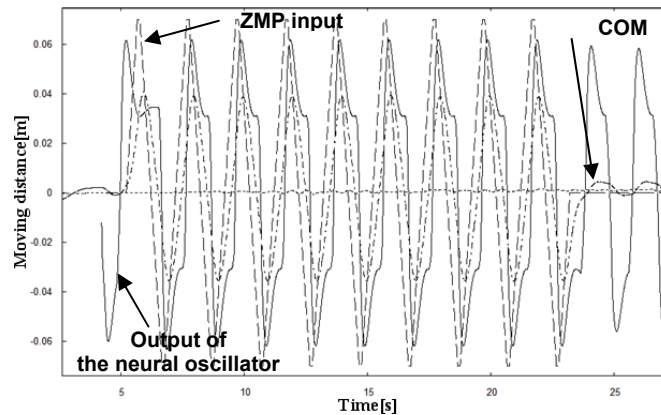


Fig. 6. Input ZMP profile (dashed line), the output of the COM position (solid line) and the output of the neural oscillator in the pitching motion (dash-dotted line)

There is the difficulty on how to or when to switch the double support phase and the single support phase under the bipedal locomotion or various humanoid behaviors. To solve this problem, we propose the proper switching rule based on the COM position and the ZMP position. Basically the balancing motion is controlled considering the only COM position. If the projected COM position in the rolling direction moves within the size of the left foot, this indicates that the left leg only supports the whole body of the humanoid robot. On the contrary, in the right leg, the single support phase becomes diametrically opposed to that. In consequence, there is the double support phase when the projected COM position is placed at inner empty

space of the size of both foots. Then both legs control the whole body of the humanoid robot.

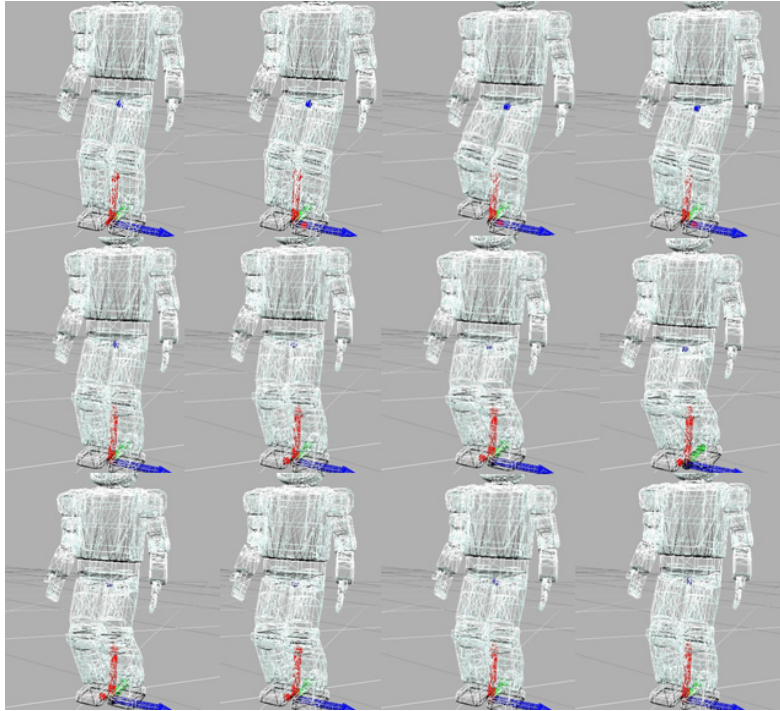


Fig. 7. Simulation result on the lifting leg motion with the transition velocity of the ZMP, 0.4cm/s.

The lifting motion of the leg is dominated in terms of the calculated ZMP position. If the ZMP position exists within the ZMP criterion of a foot, the corresponding leg can be used as the supporting leg in order to maintain the lifting motion of another leg. For instance, when the calculated ZMP position is inside the ZMP criterion of the right leg, the lifting motion of the left leg becomes possible. However, this criterion is changeable according to the moving velocity of the current ZMP position between the ZMP criterion of a foot and that of another foot. Here we should establish the condition to evaluate the performance of the bipedal walking control based on the neural oscillator coupled virtual model. The motion for keeping balance of the humanoid robot can be yielded properly in terms of the coupled model. In the simulation seen in Fig. 7, we verified the smooth and natural lifting motion regardless of the double or single support phase.

5 Experimental Verification on Human-like Whole Body Motion

5.1 Human-like Whole body Motion Generation

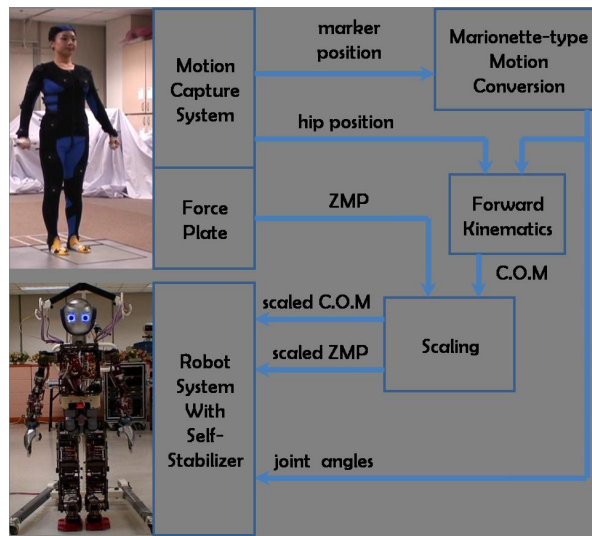


Fig. 8. Conceptual figure with respect to virtual force based motion adaptor

Figure 8 describes the conceptual virtual force based motion adaptor for the motion generation of a humanoid robot's upper body. If there is a desired motion data corresponding to each joint of the robot, the data is properly changed exploiting the marionette-type motion conversion method instead of a marker position data obtained from a motion capture system. However, in experiment, we employed a marker position data extracted from our motion capture system owing that it is difficult to create unified motions such as human-like motions. The individual joint angles and the Cartesian COM position are obtained by solving the respective forward kinematics problems. And then the ZMP position is acquired by calculating the measured data in terms of the force plate. The self-stabilizing bipedal controller drives the humanoid robot at an appropriate equilibrium point corresponding to a time-varying ZMP input, COM input and other joint motion.

Although recorded human motions can be a good means for teaching various movements to robots, they may not be applicable directly to a robot because of such geometrical and systemic differences between a human and a robot as length, degrees of freedom, and kinematics and dynamics capabilities. A marionette is a type of puppets with strings driven by a human as seen in Fig. 9. The feature of a marionette is that it is a system with passive joints and is moved by the force of strings. Applying this principle, given a robot with all passive joints, we virtually connect the position

of a human hand to that of the end-effector of the robot with an elastic strip. Then the robot follows the movement of a human arm. The movement of the robot is calculated by following forward dynamics equation.

$$M(q)\ddot{q} + V(q, \dot{q}) + G(q) + J^T F_v = \tau \quad (5)$$

where q is the joint angle vector, M is the mass matrix, V is the Coriolis vector, G includes the gravity force, τ is the joint torque vector, and J is the Jacobian matrix. As the robot has only passive joints, the joint torque is zero. F_v is the virtual force caused in terms of the elastic strip and the external force of dynamics equation.



Fig. 9. A typical marionette controlled by strings.

An elastic strip is modeled with a virtual spring and damper between the hand positions of a human and a robot. The virtual force created by elastic strip is calculated as follow:

$$F_v = k_p (x_h - x_r) + k_d (\dot{x}_h - \dot{x}_r) \quad (6)$$

where x_h , \dot{x}_h , x_r , and \dot{x}_r are the positions and velocities of the human hand and the end-effector of a robot, respectively. They are the 6-dimensional vectors including the rotation information. k_p is the spring stiffness and k_d is the damping coefficient. We are able to tune the conversion phase by changing them.

One issue of the proposed method is the effect of gravity force. When the elastic strip draws a robot at the upper position, the robot moves less than at the lower position because of gravity force. So we introduce the gravity compensation term in the joint torque instead of zero vector as follow:

$$\tau = \hat{G}(q) \quad (7)$$

where \hat{G} is the computed gravity force, which is ideally equal to G in Eq. (5) ideally.

Another issue is the joint constraint to prevent the damage of the robot. Hence, the proposed motion conversion method includes constraint conditions with respect to the individual joint angles. For this, the virtual force constraint is involved as seen in Fig. 10. If a joint has the limit q_{\max} and q_{\min} , the virtual force works as the joint angle go near its limit. The force increases exponentially when the joint angle approaches its limit.

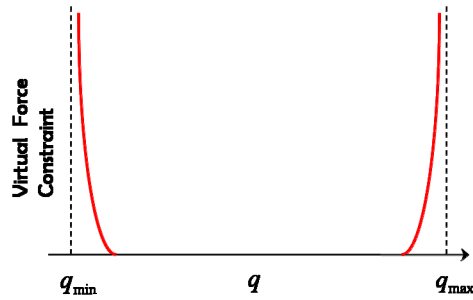


Fig. 10. Virtual force constraint.

5.2 Experimental Verification

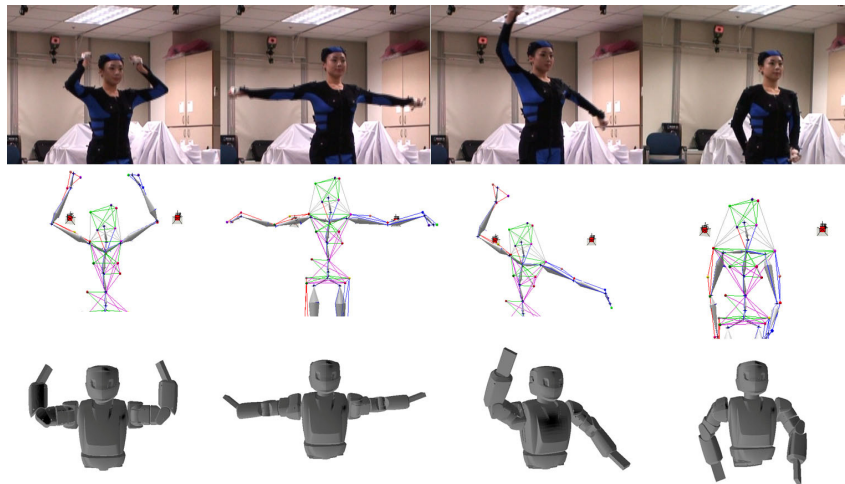


Fig. 11. The motion conversion procedure employing the marionette-type motion conversion method. The upper figures are human motion. The middle and lower figures are marker set and robot motion, respectively.

Figure 11 shows the experimental results on the motion conversion between a human

and a robot. It can be observed from the results that four representative motions of a human are well converted into a robot motion. The motion conversion process is operated fast over 100 Hz in real time. Also the virtual force led by the virtual mechanical components of the elastic strip plays on roll in noise filtering of the measured marker data such as an impedance model. So the resultant motions show smooth human-like motions.

The authors implemented the proposed control method to the real humanoid robot to verify the validities of the proposed motion adaptor with the self-stabilizing bipedal controller. The kinematic and dynamic properties of a robot such as the width of feet, the area of foot, the length and mass of leg are different from those of a human. So, considering the calculated COM, we adjust the ZMP measured from the human motion so that the bipedal stability of the humanoid robot is maintained within the stable ZMP range. It is done by just multiplication of suitable scale factor. And the modified ZMP is input to the self-stabilizing bipedal controller. Then the stable COM corresponding to the ZMP input is autonomously generated in terms of the self-stabilizing balance controller as illustrated in Fig. 3 (c). Under the dancing motion of the humanoid robot to employ the motion data obtained from the motion conversion method, unknown disturbances composed of two dumbbells of weigh 10kg are applied directly to the humanoid robot in the frontal and sagittal sides, respectively, as seen in Fig. 12. It is observed from the experiment that the humanoid robot is able to maintain the bipedal stability. Hence even though the external disturbances of a sinusoidal form effect to the humanoid robot, the humanoid robot coupled to the neural oscillator and virtual components can stably exhibit a novel adaptive motion corresponding to an unknown disturbance.

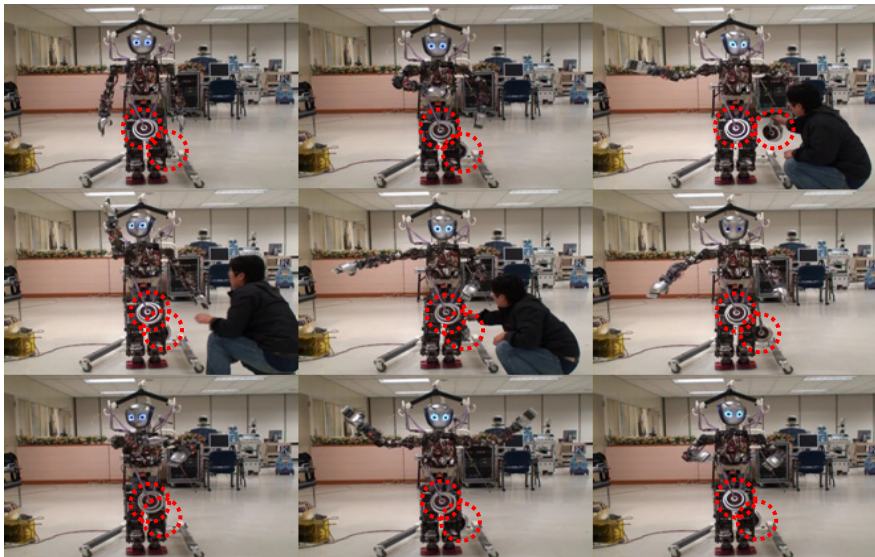


Fig. 12. Snap shots on the whole body motion and balancing test of humanoid robot under unknown disturbances, Dotted circles indicate the dumbbells employed as unknown disturbances

6 Conclusion

We have presented a new control framework for generating human-like motion of a humanoid robot. For achieving this, the end-effector of each limb of a humanoid robot is virtually connected to an elastic strip that allows a robot to exhibit human-like motion corresponding to motion captured from humans incorporating virtual forces. In addition, to attain a stable bipedal motion of humanoid robots, a new control method consisting of neural oscillators and virtual components was developed. The COM position was controlled to follow the time-varying desired ZMP input sustaining the bipedal stability, which enables a humanoid robot to maintain the bipedal stability regardless of the single or double phases even under unknown disturbances. Extensive simulations and experiments were carried out to verify the effectiveness of the proposed method. More experiments are currently under way for further evaluation of the proposed control method.

References

1. Inamura, T., Toshima, I., Tanie, H., Nakamura, Y.: Embodied Symbol Emergence Based on Mimesis Theory, *The Int. Journal of Robotics Research*, vol. 23, pp. 363-377. (2004)
2. Ijspeert, A. J., Nakanishi, J., Schaal, S.: Movement Imitation with Nonlinear Dynamical Systems in Humanoid Robots, *Proc. IEEE Int. Conf. on Robotics and Automation*, pp. 1398-1403. (2002)
3. Schaal, S.: Is Imitation Learning the Way to Humanoid Robots?, *Trends in Cognitive Science*, vol. 3, pp. 233-242. (1999)
4. Samejima, K., Katagiri, K., Doya, K., Kawato, M.: Symbolization and Imitation Learning of Motion Sequence Using Competitive Modules, *Trans. of the Institute of Electronics, Information, and Communication Engineers*, vol. J85-D-II, pp. 90-100. (2002)
5. Samejima, K., Doya, K., Kawato, M.: Inter-module Credit Assignment in Modular Reinforcement Learning, *Neural Networks*, vol. 16, pp. 985-994. (2003)
6. Nakamura, Y., Yamane, K.: Dynamics Computation of Structure-varying Kinematic Chains and Its Application to Human Figures, *IEEE Trans. on Robotics and Automation*, vol. 16, pp. 124-134. (2000)
7. Yamane, K., Nakamura, Y.: Dynamics Filter – Concept and Implementation of Online Motion Generator for Human Figures, *IEEE Trans. on Robotics and Automation*, vol. 19, pp. 421-432. (2003)
8. Yang, W., Chong, N. Y.: Goal-directed Imitation with Self-adjusting Adaptor Based on a Neural Oscillator Network, *Proc. Int. Conf. on Advanced Robotics*, pp. 404-410. (2005)
9. Yang, W., Chong, N. Y., Kim, C., You, B. J.: Locomotion Imitation of Humanoid Using Goal-directed Self-adjusting Adaptor, *Proc. IEEE/RSJ Int. Conf. on Intelligent Robots and Systems*, pp. 5650-5656. (2006)
10. Yang, W., Chong, N. Y.: Imitation Learning of Humanoid Locomotion Using the Direction of Landing Foot, *Int. Journal of Control, Automation and Systems*, to be published, (2009)
11. Vukobratovic, M., Juricic, D.: Contribution to the Synthesis of Biped Gait, *IEEE Trans. Bio-Med. Eng.*, vol. BME-16, pp. 1-6. (1969)
12. Vukobratovic, M.: How to Control Artificial Anthropomorphic Systems, *IEEE Trans. Syst., Man, Cybern.*, vol. SMC-3, pp. 497-507. (1973)

13. Kajita, S., Matsumoto, O., Saigo, M.: Real-time 3D Walking Pattern Generation for a Biped Robot with Telescopic Legs, Proc. IEEE Int. Conf. on Robotics and Automation, pp. 2299-2306. (2001)
14. Pratt, J., Chew, C.-M., Torres, Dilworth, A., P., Pratt, G.: Virtual Model Control: An Intuitive Approach for Biped Locomotion, The Int. Journal of Robotics Research, vol. 20, pp. 129-143. (2001)
15. Endo, G., Nakanishi, J., Morimoto, J., Cheng, G.: Experimental Studies of a Neural Oscillator for Biped Locomotion with QRIO, IEEE Int. Conf. on Robotics and Automation, pp. 598-604. (2005)
16. Yang, W., Chong, N. Y., Kim, C., You, B. J.: Self-adapting Humanoid Locomotion Using a Neural Oscillator Network, Proc. IEEE/RSJ Int. Conf. on Intelligent Robots and Systems, pp. 309-316. (2007)
17. Taga G., Yamagushi, Y., Shimizu, H.: Self-organized Control of Bipedal Locomotion by Neural Oscillators in Unpredictable Environment, Biological Cybernetics, vol. 65, pp. 147-159. (1991)
18. Taga, G.: A Model of the Neuro-Musculo-Skeletal System for Human Locomotion. I. Emergence of basic gait, Biological Cybernetics, vol. 73, pp. 97-111. (1995)
19. Taga, G.: A model of the neuron-musculo-skeletal system for human locomotion. II. Real-time adaptability under various constraints, Biological Cybernetics, vol. 73, pp. 113-121. (1995)
20. Yang, W., Chong, N. Y., Kim, C., You, B. J.: Entrainment-enhanced Neural Oscillator for Rhythmic Motion Control, Journal of Intelligent Service Robotics, vol. 1, pp. 303-311. (2008)
21. Arimoto, S., Sekimoto, M., Hashiguchi, H., Ozawa, R.: Natural Resolution of ill-Posedness of Inverse Kinematics for Redundant Robots: A Challenge to Bernstein's Degrees-of-Freedom Problem, Advanced Robotics, vol. 19, pp. 401-434. (2005)